TSLP Produced by *Aspergillus fumigatus*-Stimulated DCs Promotes a Th17 Response Through the JAK/STAT Signaling Pathway in Fungal Keratitis

Fang Han,[1,2] Hui Guo,[1] Leyi Wang,[1] Yuting Zhang,[1] Lin Sun,[1,2] Chenyang Dai,[1,2] and Xinyi Wu[1]

[1]Department of Ophthalmology, Qilu Hospital, Shandong University, Jinan, 250012, China
[2]The Key Laboratory of Cardiovascular Remodeling and Function Research, Chinese Ministry of Education and Chinese Ministry of Health, The State and Shandong Province Joint Key Laboratory of Translational Cardiovascular Medicine, Qilu Hospital, Shandong University, Jinan 250012, China

Correspondence: Xinyi Wu, Department of Ophthalmology, Qilu Hospital, Shandong University, 107 Wenhua Xi Road, Jinan, 250012, China;
xywu8868@163.com.

Received: August 31, 2020
Accepted: November 30, 2020
Published: December 21, 2020

Citation: Han F, Guo H, Wang L, et al. TSLP produced by *Aspergillus fumigatus*-stimulated DCs promotes a Th17 response through the JAK/STAT signaling pathway in fungal keratitis. *Invest Ophthalmol Vis Sci.* 2020;61(14):24.
https://doi.org/10.1167/iovs.61.14.24

Purpose. The purpose of this study was to explore the role of thymic stromal lymphopoietin (TSLP) secreted by *Aspergillus fumigatus*–stimulated dendritic cells (DCs) during the T helper 17 (Th17) immune response, and further clarify the mechanisms contributing to the Th17 immune response of fungal keratitis (FK).

Methods. A carboxyfluorescein diacetate succinimidyl ester assay, PCR, and flow cytometry were performed to detect Th17 differentiation of $CD4^+$ T cells; PCR, ELISA, and Western blot were used to detect the expression of TSLP and JAK/STAT–related proteins; Signaling pathways involved in Th17 response was evaluated using RNA sequence; C57BL/6 mice were infected with *A. fumigatus* and treated with ruxolitinib or BBI608. Slit-lamp examination, fluorescein staining, and clinical scores were used to assess the clinical manifestation.

Results. *A. fumigatus*–infected DCs could drive naïve $CD4^+$ T-cell proliferation and promote the production of Th17 cytokines IL-17A, IL-17F, and IL-22. *A. fumigatus* stimulation increased the expression of TSLP in DCs. DC-derived TSLP contributed to a Th17-type inflammatory response via the JAK/STAT signaling pathway. TSLP small interfering RNA, TSLPR small interfering RNA, or JAK/STAT inhibitors inhibited the Th17 immune response induced by *A. fumigatus*–infected DCs. Moreover, TSLP promoted *A. fumigatus* keratitis disease progression in a mouse model. However, inhibition of the JAK/STAT signaling pathway using a specific inhibitor reversed the development of FK by *A. fumigatus* infection.

Conclusions. TSLP secreted by *A. fumigatus*–stimulated DCs played a significant role in the Th17-dominant immune response of FK through its JAK/STAT activation. Our findings may contribute to the elucidation of the molecular mechanisms of FK and to the development of novel therapeutic approaches.

Keywords: fungal keratitis, DCs, $CD4^+$ T cells, Th17 inflammation, TSLP

Fungal keratitis (FK) is one of the most destructive corneal infections caused by pathogenic fungi, and it has high morbidity with a global distribution.[1,2] FK usually develops in people infected with pathogenic fungi such as *Aspergillus fumigatus* and *Fusarium*.[3,4] In China, the most common pathogenic fungus is the plant-associated *A. fumigatus*.[5] FK has become a major cause of blindness in many developing countries owing to the increasing use of antibiotics, poor visual prognosis, and the absence of effective symptomatic treatment.[6] Therefore, clarifying the pathogenesis of FK and developing new therapies are essential.

Both innate and adaptive immune responses participate in fungal infections of the cornea.[7] The innate immunity is the first line of host defenses to control infections.[8] After corneal infection, the pattern recognition receptors of the cornea interact with the fungal pathogen-associated molecular patterns, and initiate an innate immune response to defend the cornea against fungal pathogens. This response produces many chemokines and cytokines to recruit inflammatory cells and eliminate the pathogens, which are events that are important for maintaining the normal corneal structure.[9,10] The activated innate immunity subsequently leads to an effective adaptive immune response. Dendritic cells (DCs) are responsible for sampling antigenic material from the environment, expressing several pattern recognition receptors that recognize *A. fumigatus,* shaping T-cell responses through the secretion of cytokines, and priming T-cell responses via antigen presentation.[11,12] DCs are key regulators of immunity and the most important cells for initiating adaptive fungal immunity.[13–17]

$CD4^+$ T helper (Th) cells are crucial to the adaptive immune system.[18] After antigenic stimulation, naïve

$CD4^+$ T cells get activated, proliferate, and differentiate into cells with different effector phenotypes, including Th1, Th2, Th17, and regulatory T-cell lineages.[19] Several reports have implicated DC-derived Th17-promoting cytokines, such as IL-1β, IL-6, and IL-23, that are thought to promote Th17 responses that develop during bacterial and fungal infections.[20] However, whether an *A. fumigatus*–induced Th17 inflammatory response takes place during FK remains unknown. How DCs sense *A. fumigatus* and further induce $CD4^+$ T-cell responses also needs to be explored.

Thymic stromal lymphopoietin (TSLP) is an IL-7–related cytokine that mainly expresses in human epithelial cells in response to several stimuli, including bacteria, fungi, parasites, and inflammatory cytokines.[21] Recent studies have revealed that other types of cells such as mast cells, smooth muscle cells, fibroblasts, DCs, trophoblasts, and cancer or cancer-associated cells are also able to produce TSLP under certain inflammatory conditions.[22] TSLP is thought to mediate its biological activity through a heterodimeric receptor complex consisting of the IL-7 receptor subunit α (IL-7RA) and a TSLP-specific receptor (TSLPR).[23] The role of TSLP in the induction of the allergic Th2 immune response by DCs and the pathogenesis of allergic diseases (asthma, atopic dermatitis, and inflammatory bowel disease, and others) has been previously clarified.[24] Our initial research demonstrated that TSLP, produced by human corneal epithelial cells under the stimulation of *A. fumigatus*, could increase the proliferation of $CD4^+$ T cells, promote $CD4^+$ T cells to express IL-4 and IL-13, and finally induce a Th2 inflammatory response.[25] However, whether DCs secrete TSLP and what the role of this cytokine is in the Th17 inflammatory response that occurs during FK remain unknown.

In the present study, we seek to understand the role of TSLP secreted by *A. fumigatus*–stimulated DCs during the Th17 immune response. In addition, we aim to clarify the mechanisms contributing to the Th17 immune response of FK in vitro and in vivo.

Methods

Ethics Statement

All animal studies were approved by the Laboratory Animal Ethics Committee of Qilu Hospital of the Shandong University, and experimental conditions and treatments were in line with the guidelines of the ARVO Statement for the Use of Animals in Ophthalmic and Vision Research.

Animals, Corneal Infection, and Disease Evaluation

Wild-type C57BL/6 mice (male; age, 6–8 weeks; weight, 20–25 g) were purchased from the Laboratory Animal Center of Shandong University. Mice were anesthetized by intraperitoneal injection of pentobarbital (40 mg/kg). For corneal infection, the right cornea was wounded with three parallel 1-mm incisions using a sterilized 26G needle. A cover of parafilm M film cut with a 3-mm trephine was used as a contact lens on the surface of the scarified cornea. A fungal suspension (5 µL of a 1×10^8 pieces/mL stock) was applied to the surface of the wounded cornea and an artificial molded parafilm contact lens was placed onto the cornea. An additional 5 µL injection of fungal suspension was applied to the gap between the parafilm M film and the cornea after the eyelids had been seamed together. The left cornea treated with PBS was used as a negative control. The artificial contact lenses were removed after 12 hours and the eyes were examined at different times (0.5, 1, 3, 5, and 7 days). Clinical examinations were graded by corneal photographs, and clinical scores were calculated according to the scoring system by Wu et al.[26]

Generation and Identification of Murine Bone Marrow-Derived DCs

Bone marrow-derived DCs were isolated from the femur and tibia of 4- to 6-week-old C57BL/6 mice (both males and females) following the method of Inaba et al.[27] The cells were suspended in a 100-mm Petri dish (bacterial culture quality) and cultured in RPMI 1640 Medium (Gibco, Grand Island, NY) supplemented with 10% fetal bovine serum (FBS, Gibco), 1% penicillin/streptomycin (15140-122, Gibco), 20 ng/mL recombinant granulocyte-macrophage colony-stimulating factor (315-03, PeproTech, Rocky Hill, NJ), and 10 ng/mL IL-4 (214-14, PeproTech). A half-volume of fresh culture medium containing 20 ng/mL granulocyte-macrophage colony-stimulating factor and 10 ng/mL IL-4 was added on days 3 and 5. DCs were cultured for 7 days at 37 °C with 5% CO_2 and then stimulated with *A. fumigatus* hyphae (1×10^6 pieces/mL) for different periods.

Isolation and Stimulation of $CD4^+$ T Cells

Murine splenic $CD4^+$ T cells were purified using a negative selection Dynal $CD4^+$ T-cell isolation kit (130-104-454, Miltenyi Biotec, Bergisch Gladbach, Germany). A flow cytometry assay was performed to detect the purity of the isolated $CD4^+$ T cells. Purified naïve $CD4^+$ T cells (>95% purity) were activated with plate-bound anti-CD3 (2 µg/mL; 16-0031, Thermo Fisher, Waltham, MA) and soluble anti-CD28 (5 µg/mL; 16-0281, Thermo Fisher) for 3 days. Cells were seeded at 1×10^5 cells/well in 96-well plates and cultured in RPMI 1640 containing 10% FBS, L-glutamine (G2150, Sigma-Aldrich, St. Louis, MO), β-mercaptoethanol (M3148, Sigma-Aldrich), 1% penicillin/streptomycin, and 20 ng/mL IL-2 (214-12-100, PeproTech).

Co-culture of $CD4^+$ T Cells With DCs

For co-culture experiments, purified naïve $CD4^+$ T cells were activated by anti-CD3/CD28 for 3 days as described elsewhere in this article. DCs were seeded in 6-well plates at a density of 2×10^6 cells/well, and then stimulated with a heat-inactivated *A. fumigatus* suspension for 3 hours. Next, the activated $CD4^+$ T cells were seeded into the upper cell culture inserts with *A. fumigatus*-stimulated DCs seeded in the lower wells of a Transwell system (pore size, 0.4 µm; diameter, 24 mm; Corning, Corning, NY) and formed a nontouching co-culture unit. $CD4^+$ T cells and DCs were co-incubated at a ratio of 10:1 ($CD4^+$ T cells:DCs) for specific times. After co-culture for the indicated times, $CD4^+$ T cells in the upper inserts were collected and prepared for flow cytometry, quantitative real-time PCR, and Western blot assays.

Antibodies and Reagents

Antibodies for p-JAK1 (ab138005), p-JAK2 (ab32101), and TSLP (ab188766) were purchased from Abcam (Cambridge,

UK). β-Actin (AF5001) antibody and carboxyfluorescein diacetate succinimidyl ester (CFSE, C1031) were purchased from Beyotime (Shanghai, China). JAK1 (66466-1-Ig), JAK2 (17670-1-AP), and STAT3 (10144-2-AP) were obtained from Proteintech (Wuhan, China). p-STAT3 (9145T) antibody was purchased from CST (Danvers, MA). Antibody for RORγt (14-6988-82) was purchased from Thermo Fisher. TSLPR (SAB2900760) antibody was obtained from Sigma-Aldrich. Antibodies for APC-CD3 (100236), FITC-CD4 (100406), APC-IL-17A (506916), APC-MHC-II (107614), APC-CD80 (104714), APC-CD86 (105012), and FITC-CD11c (117306) were purchased from BioLegend (San Diego, CA). Recombinant mouse TSLP (rmTSLP) (555-TS-010) was derived from R&D System (Minneapolis, MN). Ruxolitinib (S1378) and BBI608 (S7977) were purchased from Selleck Chemicals (Houston, TX).

Flow Cytometry Assay

For the proliferation assay, extracted $CD4^+$ T cells were labeled with CFSE according to the manufacturer's protocol. The CFSE-labeled $CD4^+$ T cells were activated with rmTSLP for 4 days or co-cultured with *A. fumigatus*-stimulated DCs for 4 days, and then analyzed using a BD FACSCalibur flow cytometer. Modfit software was used for data analysis. To detect cell surface antigens of bone marrow-derived DCs and $CD4^+$ T cells, a total of 1×10^6 cells were harvested, washed with PBS, and then directly incubated with the indicated fluorescein-conjugated monoclonal antibodies (CD11c, CD86, MHC-II, CD80, IL-17A, CD4, and CD3) or isotype controls for 30 minutes at 4 °C. Subsequently, the cells were rinsed and resuspended in 500 µL PBS, and fluorescence data were collected using a BD FACSCalibur flow cytometer. The data were processed with FlowJo 10.0.7 software.

Quantitative Real-Time PCR

Total RNA was extracted from DCs and $CD4^+$ T cells with TRIzol reagent (15596018, Invitrogen). The cDNAs were synthesized using the First Strand cDNA Synthesis Kit (FSQ-101, Toyobo, Osaka, Japan) according to the manufacturer's protocol. Real-time PCR was performed using the SYBR green PCR master mix (488735200, Toyobo, Osaka, Japan) with the 7900HT Fast Real Time PCR System (Applied Biosystems, Waltham, MA). The mRNA levels of specific genes were normalized against the reference gene GAPDH using the comparative Ct method ($2^{-\Delta\Delta Ct}$). The primer pairs used are shown in the supplementary information.

ELISA

For the in vivo study, the corneas were ground using ultrasound and homogenized in 500 µL PBS supplemented with a protease inhibitor cocktail (P1005, Beyotime) and then centrifuged. For the in vitro study, DCs and $CD4^+$ T cells were treated for indicated times, and the culture supernatants were harvested and centrifuged. The production of TSLP, IL-17A, IL-17F, and IL-22 were measured with ELISA detection kits (Anoric, Tianjin, China) according to the manufacturer's instructions. All results of samples were normalized with a comparison against a standard curve and the experiments were performed in triplicate.

Western Blot

DCs and $CD4^+$ T cells were lysed in RIPA Lysis Buffer (P0013K, Beyotime) with 1 mM phenylmethanesulfonyl fluoride, and then quantified using the BCA protein assay kit (P0012, Beyotime). After separating proteins by SDS-PAGE and transferring them to PVDF membranes (Merck Millipore, Burlington, MA), the membranes were blocked in 5% nonfat dried milk for 1 hour at room temperature and incubated overnight at 4 °C with the primary antibodies. Subsequently, membranes were incubated with the appropriate secondary antibodies for 1 hour at room temperature, followed by detection using an enhanced chemiluminescence detection kit (ORT2655, PerkinElmer, Waltham, MA). To perform densitometry analysis, β-actin was used as an internal control. The relative protein levels were analyzed using the ImageJ 1.52a software.

Statistical Analysis

All cell experiments were independently repeated at least three times. For mouse experiments, each group contained at least six mice. The data were presented as the mean ± SEM and were analyzed with a one-way ANOVA using SPSS v24.0 (SPSS, Chicago, IL). Images were processed using GraphPad Prism 8.3.0 (GraphPad Software, La Jolla, CA) and Adobe Photoshop CC 20.0.5 (Adobe, San Jose, CA). Differences were considered statistically significant at a P value of less than 0.05.

Results

A. fumigatus-Stimulated DCs Induced a Th17 Inflammatory Response in $CD4^+$ T Cells

First, we identified the morphology and purity of the DCs derived from mouse bone marrow. The cells presented a typical dendritic morphology with a large number of elongated pseudopods after being cultured for 3, 5, and 7 days (Supplementary Fig. S1A). Flow cytometry assays showed that the proportion of $CD11c^+$ cells reached approximately 82.3% on average at day 5 (Supplementary Fig. S1B). The expressions of costimulatory molecules CD80, CD86, and MHC class II on the cell surfaces were increased after *A. fumigatus* stimulation (Supplementary Fig. S1C). Besides, the purity of the isolated $CD4^+$ T cells was more than 95% (Supplementary Fig. S1D). To clarify the influence of *A. fumigatus*–stimulated DCs on the proliferation of $CD4^+$ T cells, $CD4^+$ T cells were traced with the CFSE dilution method. The CFSE assay showed that *A. fumigatus*-stimulated DCs could significantly promote the proliferation of $CD4^+$ T cells (Fig. 1A and B). To investigate whether *A. fumigatus*–stimulated DCs could induce a Th17 differentiation, we used *A. fumigatus*–stimulated DCs or nonstimulated DCs to differentiate naïve $CD4^+$ T cells into Th cells in co-culture systems. After 4 days of co-culture, the qRT-PCR results showed that *A. fumigatus*-stimulated DCs induced $CD4^+$ T-cell differentiation into Th cells that expressed IL-17A, IL-17F, and IL-22, which are features of Th17 polarization (Fig. 1C). Flow cytometry assay showed that the level of IL-17A in $CD4^+$ T cells infected with *A. fumigatus*–stimulated DCs was markedly increased compared with that in the control group (Fig. 1D and E). Collectively, these results suggest that the Th17 inflammatory response

Investigative Ophthalmology & Visual Science

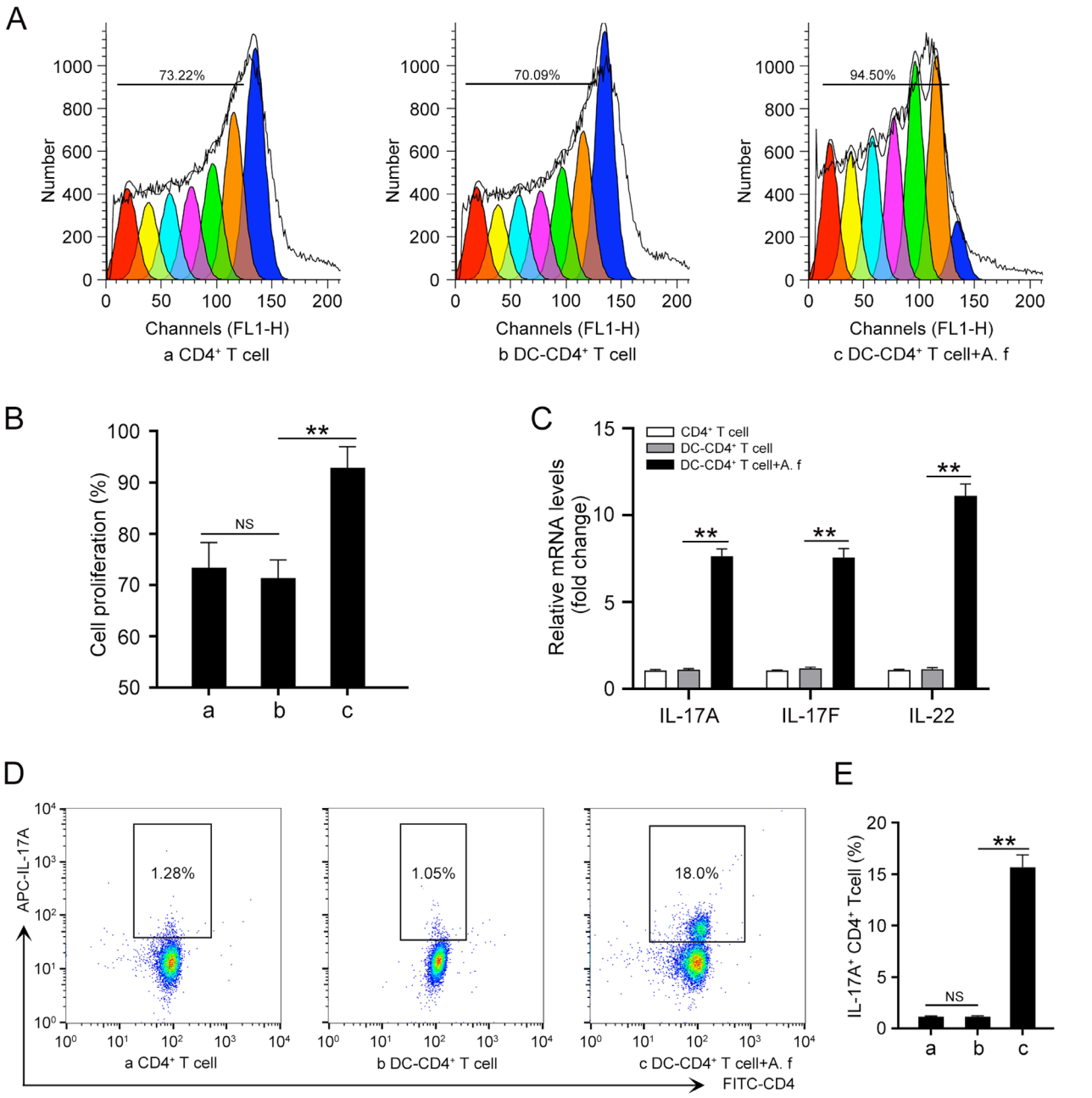

Figure 1. *A. fumigatus*–stimulated DCs promotes Th17 inflammatory response. Cells were divided into three groups: (a) $CD4^+$ T cell; (b) DCs co-cultured with $CD4^+$ T cells for 4 days (DC–$CD4^+$ T cell); and (c) DCs were stimulated with heat-killed *A. fumigatus* hyphae (1×10^6 pieces/mL) for 3 hours and then co-cultured with $CD4^+$ T cells for 4 days (DC-$CD4^+$ T cell+A. f). (A) CFSE was conducted to detect cell proliferation of $CD4^+$ T cells. (B) Quantification of the cell proliferation rate in (A). (C) qRT-PCR was performed to assess the mRNA levels of IL-17A, IL-17F, and IL-22 in $CD4^+$ T cells. (D) Protein levels of IL-17A were detected by flow cytometry. (E) Quantification of IL-17A levels in (D). (Data are mean ± SEM, $^*P < 0.05$, $^{**}P < 0.01$, $n = 3$).

was induced in $CD4^+$ T cells when co-cultured with *A. fumigatus*–stimulated DCs.

A. fumigatus Enhanced TSLP Expression in DCs

To detect the expression of TSLP in *A. fumigatus*-stimulated DCs, DCs were treated with heat-killed *A. fumigatus* hyphae (1×10^6 pieces/mL) for 1, 3, 6, 12, 24, and 48 hours. The qRT-PCR (Fig. 2A) and ELISA (Fig. 2B) assay results showed that the expression of TSLP was increased at 1, 3, 6, 12, 24, and 48 hours in DCs after *A. fumigatus* infection. Consistently, Western blot results showed that the TSLP protein levels in the same DCs were also increased in a time-dependent manner (Fig. 2C). Furthermore, DCs were treated with heat-killed *A. fumigatus* hyphae for 12 hours, and then subjected to immunofluorescence analysis for TSLP. The result confirmed that DCs expressed more TSLP in response to *A. fumigatus* stimulation than in their nonstimulated state (Fig. 2D). Another group of DCs was transfected with TSLP small interfering RNA (siRNA) to verify the specificity of the TSLP antibody we used (Fig. 2D).

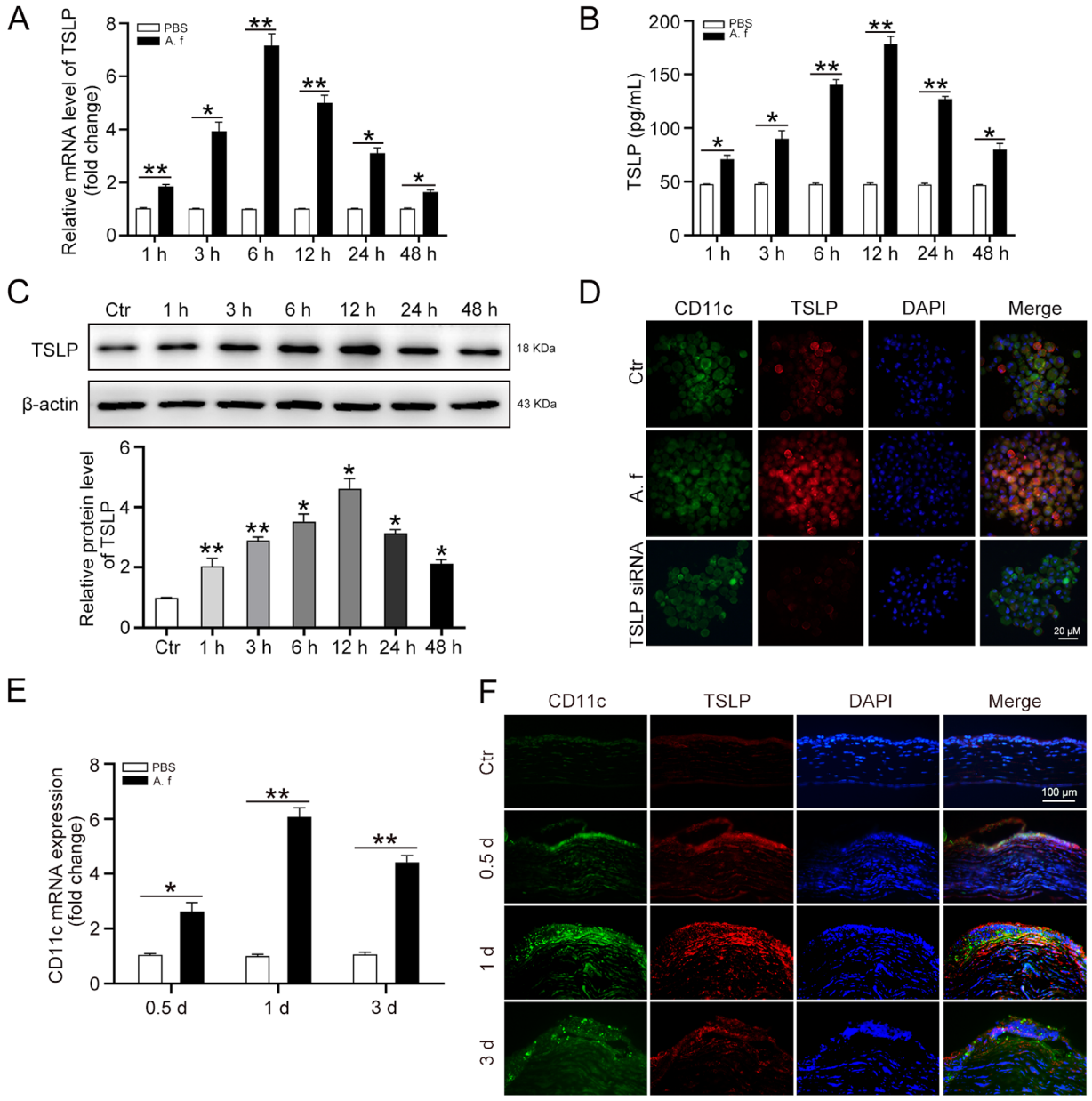

Figure 2. *A. fumigatus* hyphae induces TSLP expression in DCs. DCs were stimulated with heat-killed *A. fumigatus* hyphae (1×10^6 pieces/mL) for 1, 3, 6, 12, 24, and 48 hours. (A) qRT-PCR and (B) ELISA were performed to analyze the mRNA and protein levels of TSLP. (C) Protein levels of TSLP in DCs were detected by Western blot. (D) DCs were transfected with TSLP siRNA (80 nM) for 48 hours or treated with heat-killed *A. fumigatus* hyphae for 12 hours, then subjected to immunofluorescence analysis of TSLP (red) and CD11c (*green*). Scale bar = 20 μM. C57BL/6 mice corneas were scratched with 26G needles followed by treatment with *A. fumigatus* for 0.5, 1, and 3 days. (E) qRT-PCR was used to assess CD11c mRNA levels in mouse corneas. (F) Immunofluorescence analysis of CD11c and TSLP co-staining on the cornea at 0.5, 1, and 3 days after *A. fumigatus* infection. Nuclei were counterstained with DAPI (*blue*). The CD11c and TSLP co-staining presented the bright yellow fluorescent light. Scale bar = 100 μM. (Data are mean ± SEM, $^*P < 0.05$, $^{**}P < 0.01$, $n = 3$; for mouse, $n = 6$).

To monitor the disease progression of *A. fumigatus*–infected corneas, mice corneas were examined under slit-lamp photography and clinical scoring at 0 (control), 0.5, 1, 3, 5, and 7 days after infection to estimate the disease severity. Typical lesions of early stage corneal fungal infection, such as corneal edema or epithelial coloboma, were present in corneal epithelia at 0.5 days after infection. These corneal injuries continued to develop at 1 day after infection, and epithelial lesions began to decrease at 3 days after infection (Supplementary Fig. S2A and B). To determine whether DCs were involved in *A. fumigatus* infection, we measured the expression of CD11c, a defining marker for DCs. The qRT-PCR results demonstrated that the mRNA level of CD11c was increased at 0.5, 1, and 3 days after infection in the infected corneas (Fig. 2E). Immunofluorescence assay images also showed that *A. fumigatus* infection enhanced CD11c and TSLP expressions both in epithelium and stroma at 0.5 and 1 day post infection (Fig. 2F). Therefore, these data indicate that *A. fumigatus* stimulation increased the expression and secretion of TSLP in DCs.

Investigative Ophthalmology & Visual Science

TSLP Increased the Proliferation of CD4$^+$ T Cells and the Expression of Th17 Cytokines

Considering the upregulation of TSLP in *A. fumigatus*–infected DCs, we then turned to investigate the influence of TSLP on naïve CD4$^+$ T-cell differentiation. First, we determined whether TSLP could increase the proliferation of CD4$^+$ T cells; we stained cells with CFSE and stimulated them with 100 ng/mL rmTSLP or with a negative control solution for 4 days, and surveyed them using a flow cytometry assay. The results showed that TSLP stimulated CD4$^+$ T-cell proliferation compared with cells cultured without rmTSLP (Fig. 3A and B). The qRT-PCR (Fig. 3C) and ELISA (Fig. 3D) results suggest that the expression of IL-17A, IL-17F, and IL-22 was increased at 1, 2, and 3 days in CD4$^+$ T cells treated with rmTSLP. Moreover, a flow cytometry assay showed that TSLP promoted CD4$^+$ T cells to express more IL-17A in a time-dependent manner (Fig. 3E and F). Our results indicate that TSLP promoted a Th17 inflammatory response by CD4$^+$ T cells.

Th17 Inflammatory Response Induced by *A. fumigatus*-Stimulated DCs Was Dependent on TSLP

Next, we determined whether *A. fumigatus*-stimulated DCs promoted the Th17 inflammatory response through TSLP. DCs were incubated with negative control (NC) siRNA or TSLP siRNA (80 nM) for 48 hours, and then were stimulated with *A. fumigatus* or grown without the inactivated fungi for 12 hours. TSLP depletion efficiency was detected by qRT-PCR. The results showed that TSLP was deleted 80% by TSLP siRNA compared with the TSLP amount in NC siRNA-treated cells (Fig. 4A). The knockdown efficiency of TSLP was also confirmed by Western blot (Fig. 4B). To clarify the influence of TSLP on CD4$^+$ T-cell proliferation, DCs were transfected with NC siRNA or TSLP siRNA, challenged with *A. fumigatus* hyphae, and then co-cultured with CFSE-stained CD4$^+$ T cells for 4 days. Flow cytometry results showed that the increased proliferative response of CD4$^+$ T cells was interrupted by the knockdown of TSLP in the DCs (Fig. 4C and D). The mRNA levels of IL-17A, IL-17F, and IL-22 were also decreased in the TSLP siRNA-treated group compared with the levels in the NC siRNA treated group (Fig. 4E). In addition, the knockdown of TSLP downregulated IL-17A production compared with the NC siRNA treated group (Fig. 4F).

To elucidate the role of the TSLPR in the Th17 response induced by *A. fumigatus*–stimulated DCs, we treated CD4$^+$ T cells with TSLPR siRNA (80 nm) for 24 hours, then co-cultured them with *A. fumigatus*–stimulated DCs for 4 days. The results showed that *A. fumigatus*–stimulated DCs failed to increase the mRNA levels of IL-17A, IL-17F, and IL-22 in CD4$^+$ T cells with TSLPR knockdown (Supplementary Fig. S3C and D, Fig. 4G). In addition, the protein level of IL-17 was significantly lower in the TSLPR knockdown group than those observed in the control group (Fig. 4H). These data suggest that *A. fumigatus*–stimulated DCs promoted the Th17 inflammatory response of CD4$^+$ T cells through TSLP.

High-throughput Sequencing Assay of Signaling Pathways in the Th17 Response of CD4$^+$ T Cells

To analyze the signaling pathways that participated in the Th17 response of CD4$^+$ T cells during *A. fumigatus* infection, we performed RNA sequencing to detect the differences in mRNA expression between CD4$^+$ T cells co-cultured with *A. fumigatus*–stimulated DCs or grown by themselves. We identified 1273 upregulated and 986 downregulated differentially expressed genes between DC–CD4$^+$ T cells and DC–CD4$^+$ T cells plus *A. fumigatus* (Fig. 5A). Kyoto Encyclopedia of Genes and Genomes results showed that JAK/STAT was the most remarkable signaling pathway in CD4$^+$ T cells co-cultured with *A. fumigatus*–stimulated DCs (Fig. 5B and C). We verified the mRNA expression profile involved in the JAK/STAT signaling pathway obtained by high-throughput sequencing using qRT-PCR in DC–CD4$^+$ T cells and DC–CD4$^+$ T cells plus *A. fumigatus* (Fig. 5D). Our results indicate that the JAK/STAT signaling pathway might play an important role in the Th17 response of CD4$^+$ T cells.

A. fumigatus–Stimulated DCs Activated the JAK/STAT Signaling Pathway Through TSLP Secretion

Based on the RNA sequencing results suggesting that the JAK/STAT signaling pathway is activated during the *A. fumigatus*-induced Th17 response of CD4$^+$ T cells, we investigated whether *A. fumigatus*–stimulated DCs activated the JAK/STAT signaling pathway in CD4$^+$ T cells. Our results showed that the phosphorylation levels of JAK1, JAK2, and STAT3, key molecules of the JAK/STAT signaling cascade were high in CD4$^+$ T cells co-cultured with *A. fumigatus*–infected DCs. Moreover, *A. fumigatus*–infected DCs also enhanced the expression of RORγt, which acted as a downstream transcription factor of the JAK/STAT signaling pathway and promoted Th17 cell differentiation (Fig. 6A and C). Consistently, we observed the activation of the JAK/STAT signaling pathway in CD4$^+$ T cells stimulated with rmTSLP for 3 days (Fig. 6B and D). To further confirm the role of TSLP in the activation of the JAK/STAT signaling pathway in CD4$^+$ T cells, DCs transfected either with NC siRNA or with TSLP siRNA were stimulated with *A. fumigatus* hyphae and then co-cultured with CD4$^+$ T cells for 4 days. The Western blot results showed that the expression of RORγt, p-JAK1, p-JAK2, and p-STAT3 was significantly decreased in TSLP siRNA-transfected DCs compared with the levels in NC siRNA-transfected DCs (Fig. 6E). Moreover, *A. fumigatus*–infected DCs failed to promote the protein levels of RORγt, p-JAK1, p-JAK2, and p-STAT3 in CD4$^+$ T cells incubated with TSLPR siRNA (Fig. 6F). Taken together, these results indicate that TSLP mediated the activation of the JAK/STAT signaling pathway in CD4$^+$ T cells evoked by *A. fumigatus*–stimulated DCs.

A. fumigatus–Stimulated DCs Promoted a Th17 Response in CD4$^+$ T Cells via the JAK/STAT Signaling Pathway

We next determined whether the activation of the JAK/STAT signaling pathway was involved in the Th17 inflammatory response induced by *A. fumigatus*-infected DCs. Different concentrations (5, 10, 100, and 300 nM) of ruxolitinib, a selective inhibitor of JAK1/JAK2,[28] were used to inhibit JAK1/2. The results from Western blotting showed that 100 nM ruxolitinib could effectively suppress the phosphorylation of JAK1/2 (Supplementary Fig. S4A). Similarly, 3 µM BBI608, a specific inhibitor of STAT3,[29] was used to disrupt the function of STAT3 (Supplementary Fig. S4B). Our data

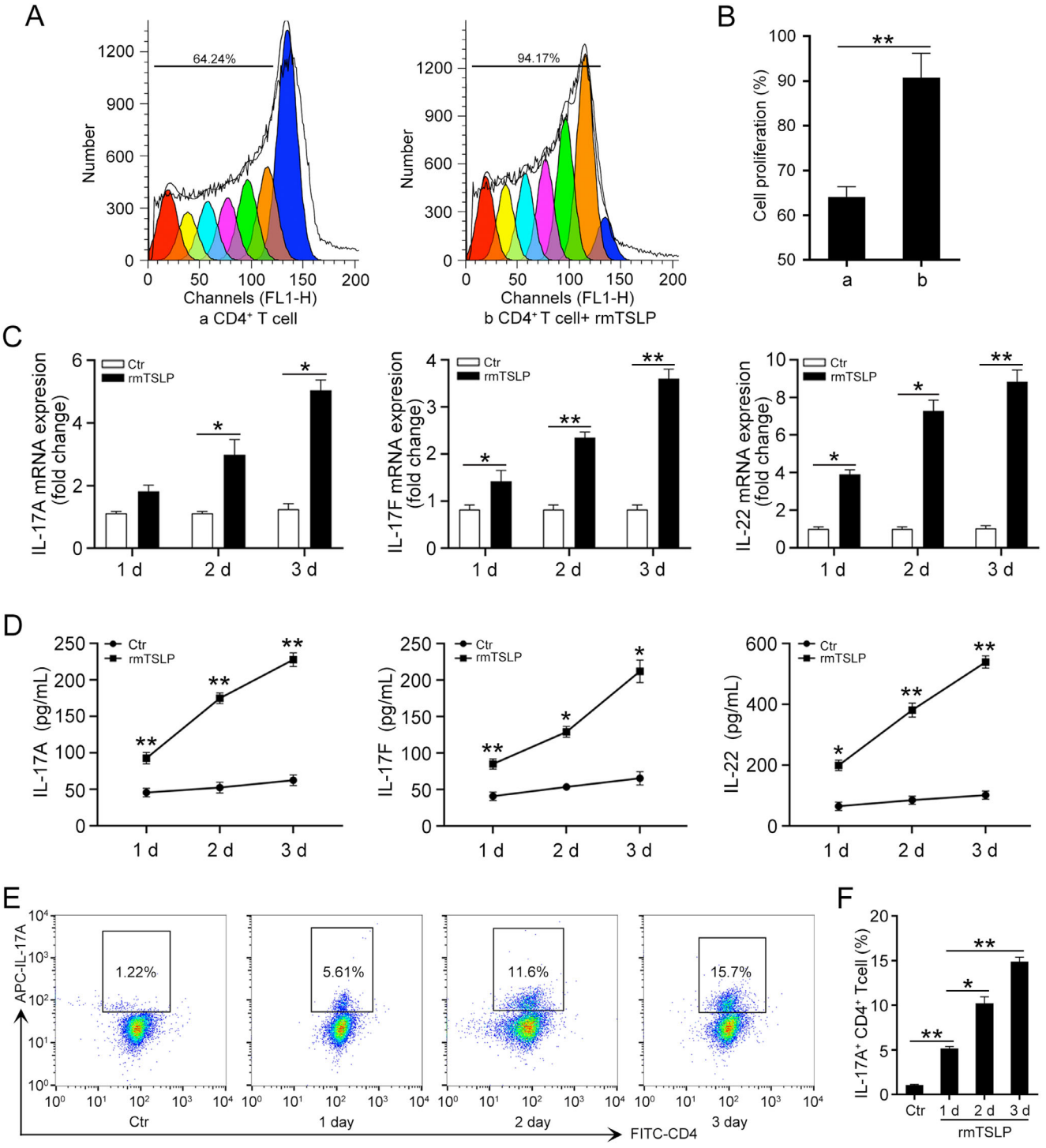

Figure 3. TSLP promotes $CD4^+$ T cell proliferation and Th17 cytokine expression. (A) $CD4^+$ T cells were stained with CFSE and then cultured with or without 100 ng/mL rmTSLP for 4 days, flow cytometry was performed to detect the proliferation of $CD4^+$ T cells. (B) Quantification of cell proliferation rate in (A). $CD4^+$ T cells were cultured with rmTSLP (100 ng/mL) for 1, 2, and 3 days. (C) qRT-PCR and (D) ELISA were performed to detect the mRNA and protein levels of IL-17A, IL-17F, and IL-22 in $CD4^+$ T cells. (E) Flow cytometry was conducted to analyze the protein levels of IL-17A in $CD4^+$ T cells. (F) Quantification of IL-17A levels in (E). Ctr, control. (Data are mean ± SEM, $^*P < 0.05$, $^{**}P < 0.01$, $n = 3$).

showed that the inhibition of the JAK/STAT signaling pathway with ruxolitinib or BBI608 effectively abrogated the increased protein levels of IL-17A in $CD4^+$ T cells induced by *A. fumigatus*–infected DCs (Fig. 7A and B). Consistently, the increased mRNA levels of IL-17A, IL-17F, and IL-22 were also disrupted with ruxolitinib or BBI608 treatment in $CD4^+$ T cells co-cultured with *A. fumigatus*–stimulated DCs (Fig. 7C). Moreover, flow cytometry analysis showed a reduction of IL-17A expression in $CD4^+$ T cells treated with rmTSLP in the presence of ruxolitinib or BBI608 (Fig. 7D and E). The

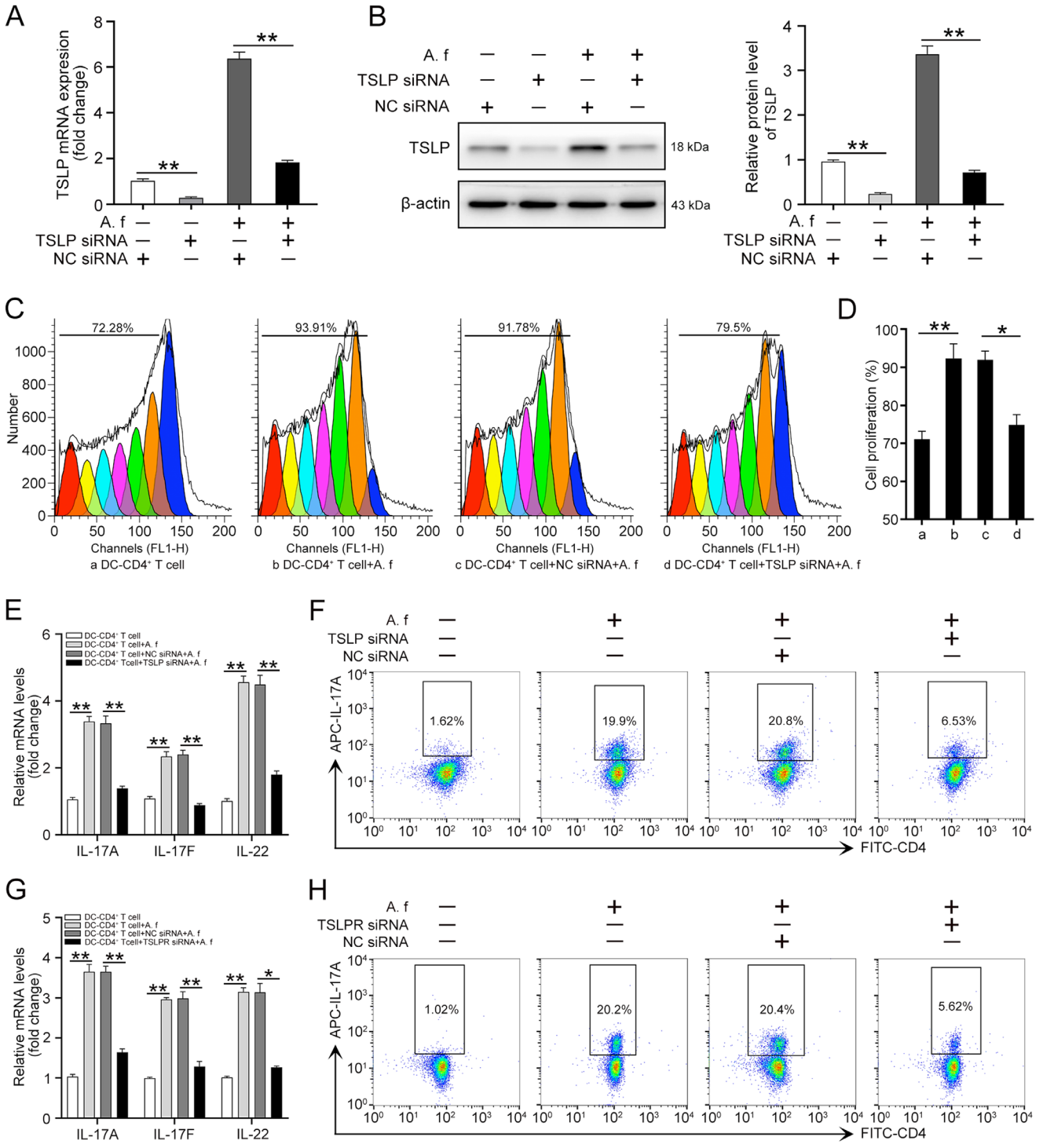

Figure 4. *A. fumigatus*–stimulated DCs promotes the Th17 response of $CD4^+$ T cells through TSLP. DCs were incubated with NC siRNA or TSLP siRNA (80 nM) for 48 hours, then stimulated with or without *A. fumigatus* for 12 hours. (A) Total RNA was isolated from DCs to assess the mRNA level of TSLP. (B) Western blot was used to analyze the protein level of TSLP. To co-culture with $CD4^+$ T cell, four types of DCs were applied: (a) DCs treated with culture medium; (b) DCs stimulated with *A. fumigatus* hyphae (A. f); (c) DCs treated with NC siRNA followed by stimulated with *A. fumigatus* hyphae (NC siRNA+A. f); d) TSLP knockdown DCs stimulated with *A. fumigatus* hyphae (TSLP siRNA+A. f). After incubated with NC siRNA or TSLP siRNA (80 nM) for 24 hours, *A. fumigatus*-stimulated DCs were co-cultured with $CD4^+$ T cells for 4 days. (C) CFSE was conducted to detect cell proliferation of $CD4^+$ T cells. (D) Quantification of cell proliferation rate in (C). (E) qRT-PCR was used to detect the mRNA levels of IL-17A, IL-17F, and IL-22 in $CD4^+$ T cells. (F) Flow cytometry was performed to detect the protein levels of IL-17A in $CD4^+$ T cells. Quantification of IL-17A level was shown in Supplementary Figure S3A. $CD4^+$ T cells were incubated with TLSPR siRNA (80 nM) or NC siRNA for 24 hours, then co-cultured with *A. fumigatus*–stimulated DCs for 4 days. (G) qRT-PCR was performed to detect the mRNA levels of IL-17A, IL-17F, and IL-22 in $CD4^+$ T cells. (H) Flow cytometry was performed to detect the protein levels of IL-17A in $CD4^+$ T cells. Quantification of IL-17A level was shown in Supplementary Figure S3B. (Data are mean ± SEM, $^*P < 0.05$, $^{**}P < 0.01$, $n = 3$).

Investigative Ophthalmology & Visual Science

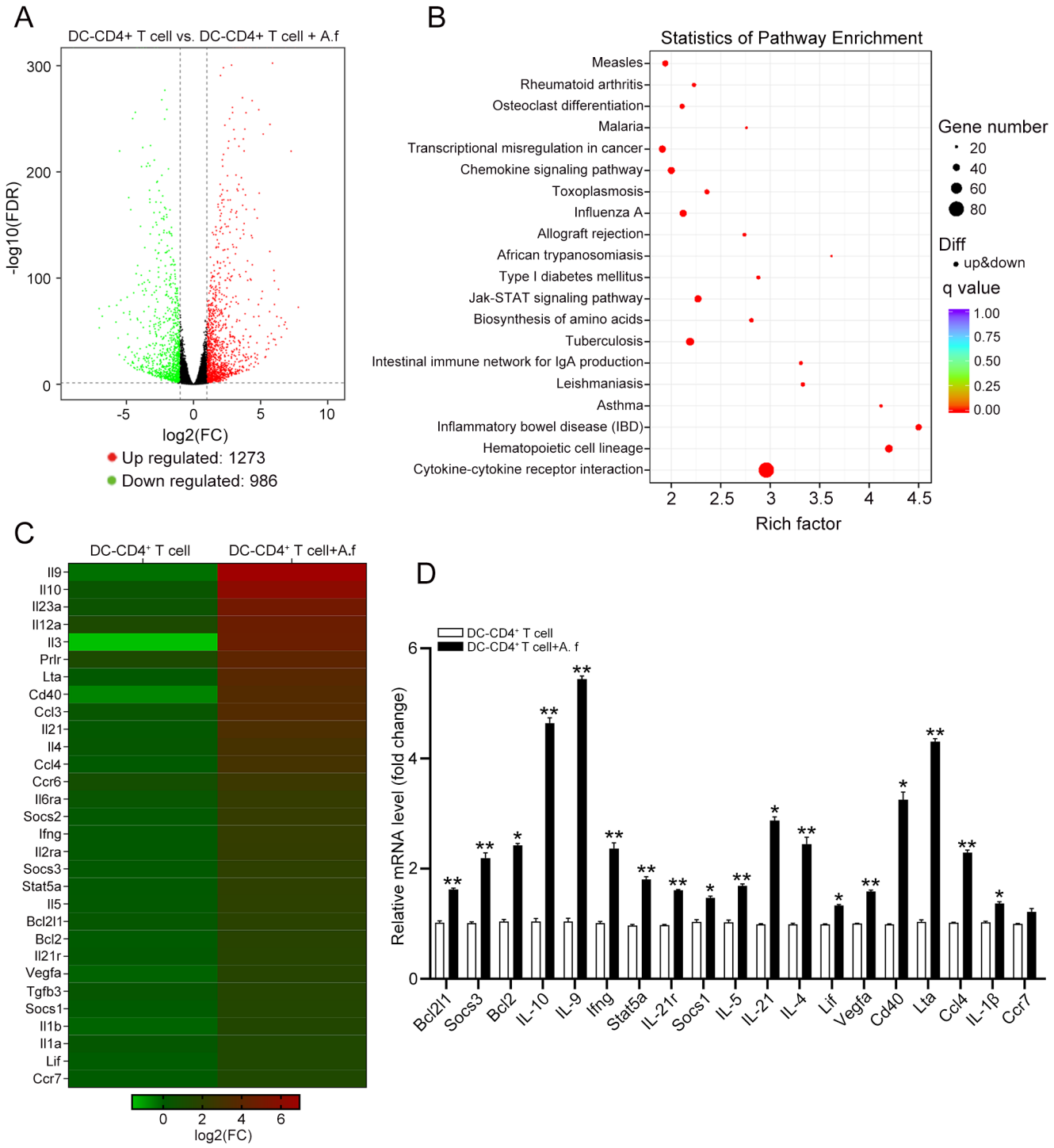

Figure 5. A next-generation sequencing analysis of the signaling pathways in the Th17 response of $CD4^+$ T cell. DCs were stimulated with *A. fumigatus* and then co-cultured with $CD4^+$ T cells for 4 days. A high-throughput RNA sequencing analysis was conducted to determine the mRNA expression profile of $CD4^+$ T cells. (A) A volcano plot revealed the differentially expressed genes (DEGs) in DC-$CD4^+$ T cell and DC-$CD4^+$ T cell+A. f groups. (B) Pathway analysis of DEGs based on the Kyoto Encyclopedia of Genes and Genomes database. (C) A heatmap of DEGs in JAK/STAT signaling pathway between DC-$CD4^+$ T cell and DC-$CD4^+$ T cell+A. f groups. (D) A qRT-PCR verification of representative DEGs between the above two groups. (Data are mean ± SEM, $^*P < 0.05$, $^{**}P < 0.01$, $n = 3$).

mRNA levels of IL-17A, IL-17F, and IL-22 were also decreased in response to ruxolitinib or BBI608 in $CD4^+$ T cells treated with rmTSLP (Fig. 7F). Therefore, these results suggest that *A. fumigatus*–stimulated DCs promoted the Th17 response of $CD4^+$ T cells via the JAK/STAT signaling pathway.

TSLP Promoted FK Progression Through JAK/STAT

Given the significance of TSLP and JAK/STAT in the Th17 response induced by *A. fumigatus*–stimulated DCs, we

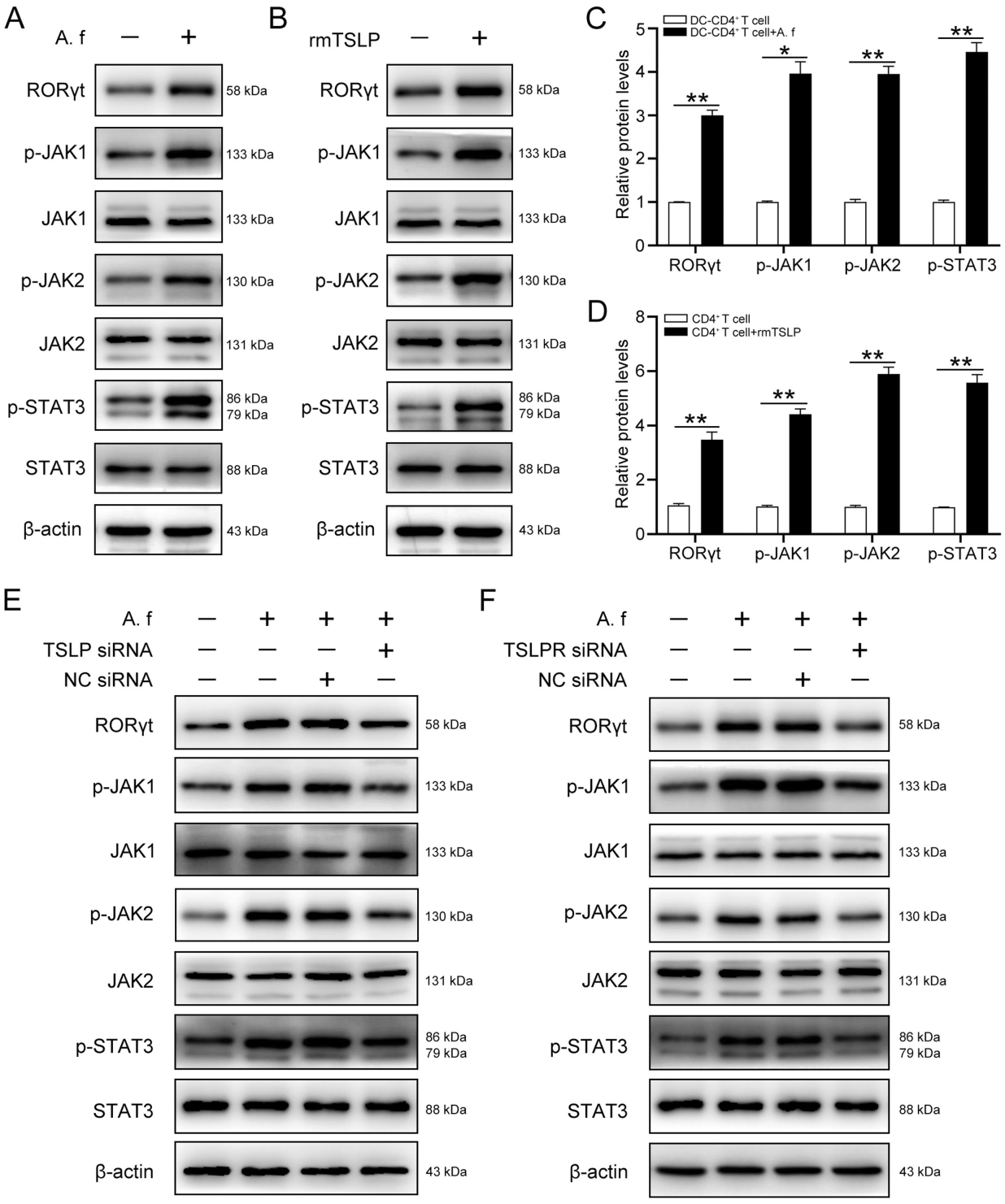

Figure 6. *A. fumigatus*–stimulated DCs activates JAK/STAT through TSLP. (A) DCs were treated with *A. fumigatus* and then co-cultured with $CD4^+$ T cells for 4 days, a Western blot analysis was performed to determine the protein levels of RORγt, p-JAK1, JAK1, p-JAK2, JAK2, p-STAT3, STAT3, and β-actin in the $CD4^+$ T cells. (B) $CD4^+$ T cells were cultured with rmTSLP (100 ng/mL) for 3 days, protein levels of RORγt, p-JAK1, JAK1, p-JAK2, JAK2, p-STAT3, STAT3, and β-actin were analyzed by western blot. Quantification of relative protein levels in (A) and (B) were shown in (C) and (D), respectively. Cells were divided into four groups and were treated as described in Figure 4C. (E) Western blot analysis of the protein levels of RORγt, p-JAK1, JAK1, p-JAK2, JAK2, p-STAT3, STAT3, and β-actin in $CD4^+$ T cells. (F) $CD4^+$ T cells were incubated with TLSPR siRNA (80 nM) or NC siRNA for 24 hours, then co-cultured with *A. fumigatus*–stimulated DCs for 4 days. A Western blot was performed to detect the protein levels of RORγt, p-JAK1, JAK1, p-JAK2, JAK2, p-STAT3, STAT3, and β-actin in $CD4^+$ T cells. Quantification of relative protein levels in (E) and (F) were shown in Supplementary Figure S4C and D. (Data are mean ± SEM, $^*P < 0.05$, $^{**}P < 0.01$, $n = 3$).

Investigative Ophthalmology & Visual Science

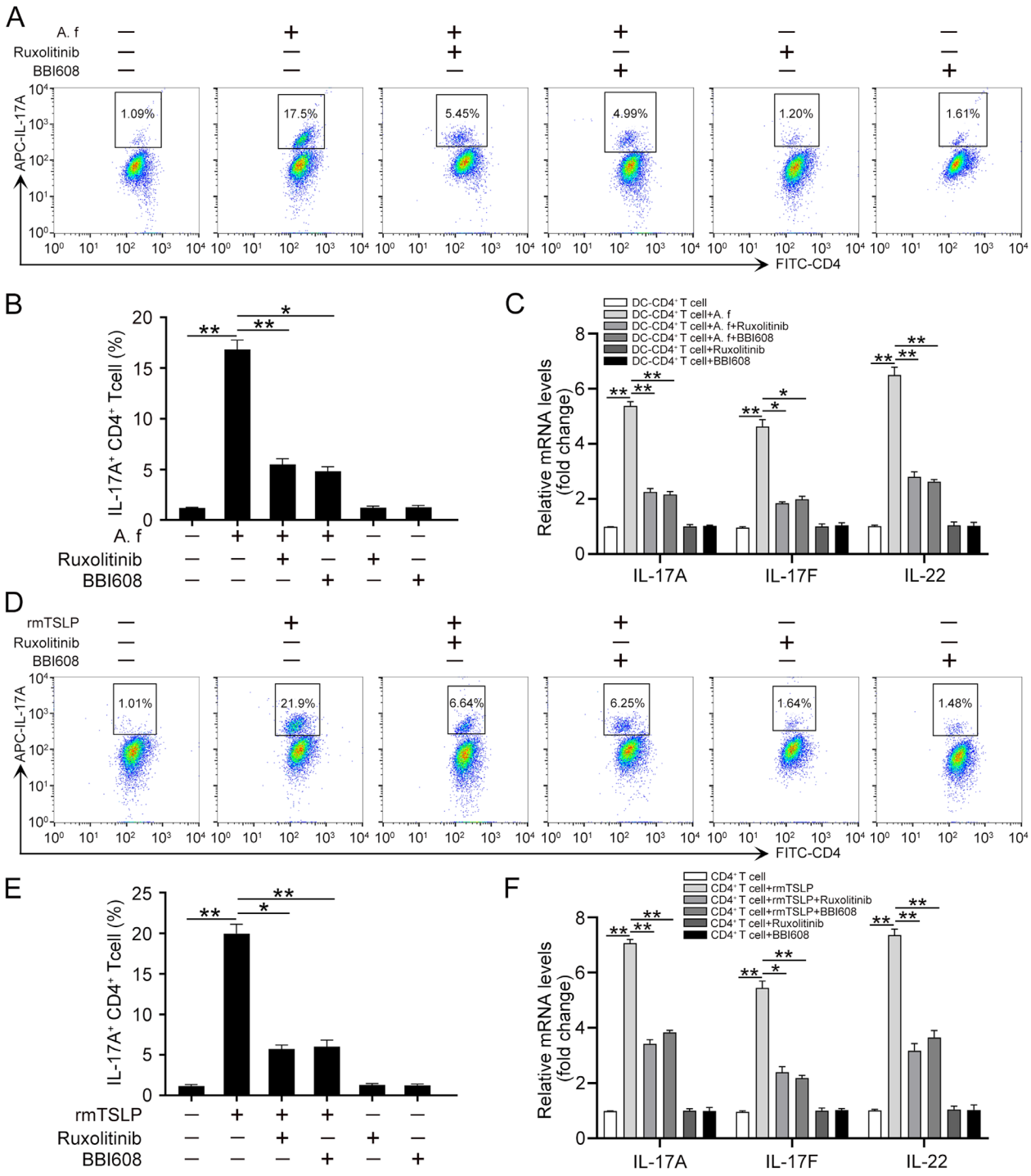

Figure 7. *A. fumigatus*–stimulated DCs promotes Th17 response of $CD4^+$ T cell via JAK/STAT. $CD4^+$ T cells were co-cultured with *A. fumigatus*–stimulated DCs in the presence or absence of ruxolitinib (100 nM) or BBI608 (3 µM) for 4 days. (A) Flow cytometry was conducted to analyze the protein levels of IL-17A in $CD4^+$ T cells. (B) Quantification of IL-17A levels in (A). (C) qRT-PCR was performed to detect the mRNA levels of IL-17A, IL-17F, and IL-22 in $CD4^+$ T cells. The $CD4^+$ T cells were treated with or without rmTSLP (100 ng/mL), ruxolitinib (100 nM), and BBI608 (3 µM) for 3 days. (D) Flow cytometry was conducted to analyze the protein levels of IL-17A in $CD4^+$ T cells. (E) Quantification of IL-17A levels in (D). (F) qRT-PCR was performed to detect the mRNA levels of IL-17A, IL-17F, and IL-22. (Data are mean ± SEM, $^*P < 0.05$, $^{**}P < 0.01$, $n = 3$).

decided to further study the role of TSLP and JAK/STAT signaling in *A. fumigatus*–infected corneas with FK. To clarify the role of TSLP in *A. fumigatus*–infected corneas, we pretreated mice by subconjunctival injection with BSA, rmTSLP, NC siRNA, or TSLP siRNA before infection with *A. fumigatus* hyphae. The corneal injury degree was determined by clinical scoring at 1 day after infection. These results suggested that corneal damages, including keratitis, necrosis, and epithelial edema, were enhanced in the group treated with rmTSLP, whereas the injuries were less severe in

Investigative Ophthalmology & Visual Science

the TSLP siRNA group at 1 day after infection (Fig. 8A and B). The qRT-PCR results showed that the TSLP levels in the TSLP siRNA group were knocked down to approximately 75% of the normal level seen in the NC siRNA group (Fig. 8C). The mRNA and protein levels of Th17 cytokines (IL-17A, IL-17F, and IL-22) were evidently decreased in TSLP siRNA-treated corneas compared with the levels in the NC siRNA-treated corneas. However, by comparison, we observed a significant increase in IL-17A, IL-17F, and IL-22 mRNA and protein levels in the mouse corneas with rmTSLP treatment (Fig. 8D and E). To investigate the function of JAK/STAT in FK, we subconjunctivally injected the mouse corneas with PBS (control), ruxolitinib, or BBI608 before treatment with *A. fumigatus* hyphae for 1 day. The corneas showed a severe cellular infiltration with destruction of the corneal epithelium stroma 1 day after *A. fumigatus* infection, whereas the corneal inflammatory response was significantly alleviated in the ruxolitinib or BBI608 injected group (Fig. 8F). The average clinical scores of the ruxolitinib or BBI608-treated corneas were also lower than those of ordinary infected corneas (Fig. 8G). Consistently, we observed that the mRNA levels and protein secretions of Th17 cytokines (IL-17A, IL-17F, and IL-22) were evidently reduced in the ruxolitinib or BBI608 injected group (Fig. 8H and I). Taken together, our results suggest that TSLP promoted the disease progression of *A. fumigatus* keratitis. However, inhibition of the JAK/STAT signaling pathway reversed the development of FK.

Discussion

FK is a severe infective corneal disease caused by pathogenic fungi; it continues to be an important cause of corneal blindness with global distribution owing to its rapid progression, poor prognosis, and absence of effective symptomatic treatment.[6] However, the underlying mechanisms of FK remain obscure. Therefore, understanding the specific mechanisms and identifying effective therapeutic targets for FK is of enormous clinical significance. In the current study, we demonstrated that *A. fumigatus* promoted TSLP expression in DCs; DC-derived TSLP induced the activation of $CD4^+$ T cells and contributed to mounting a Th17-type inflammatory response via JAK/STAT signaling in vitro and in vivo.

Th17 cells are potent inducers of tissue inflammation and have been implicated in the pathogenesis of many experimental autoimmune diseases and human inflammatory conditions. Previous studies have demonstrated that mice infected with *Cryptococcus neoformans* could develop protective Th17-type T-cell responses.[30] Wan et al.[31] report that regulatory T cells and Th17 cells display complicated interplays during viral infections: Th17 cells contribute to immune activation and disease progression, whereas regulatory T cells inhibit this process and play a key role in the maintenance of immune homeostasis. *Pseudomonas aeruginosa* infection induces a strong Th17-mediated corneal pathology, and application of Galectin-1 diminishes corneal lesion severity by inhibition of Th17 responses.[32] *Aspergillus* and *Fusarium* corneal infections are regulated by Th17 cells and IL-17–producing neutrophils, which are proven to participate in the growth of fungal hyphae and the severity of corneal disease.[33] A study from human corneal tissues infected with *Aspergillus* or *Fusarium* shows that IL-17 expression is elevated compared with uninfected donor corneas.[34] Previous data from our laboratory demonstrated that *A. fumigatus* can promote Th2 inflammation of human corneal epithelial cells.[25] We further proved that TSLP-activated DCs induce Th2 inflammation in *A. fumigatus* keratitis.[35] However, relatively little is known about the immune mechanism that drives the induction of the Th17 inflammatory response in FK. In the present study, we found that *A. fumigatus*–stimulated DCs could significantly promote the proliferation of $CD4^+$ T cells. Moreover, *A. fumigatus*–stimulated DCs could stimulate $CD4^+$ T cells to produce large amounts of Th17-type cytokines. These results show that *A. fumigatus*–stimulated DCs could induce a Th17 inflammatory response of $CD4^+$ T cells, which promoted the progression of FK.

The cytokine TSLP has been demonstrated to play important roles in maintaining immune homeostasis and regulating inflammatory responses. Previous studies have reported that TSLP can strongly activate DCs and produce several phenotypic changes, including improved survival, upregulation of MHC class II, and the production of a variety of chemokines.[22,36] Our previous studies showed that *A. fumigatus*–stimulated human corneal epithelial cells to express more TSLP, which further increased the proliferation of $CD4^+$ T cells and induced Th2 inflammation to participate in adaptive immunity.[25] However, the relationship between DC-derived TSLP and Th17 inflammation in FK has not been reported. In this study, we found that $CD4^+$ T cells produced large amounts of Th17-type cytokines and showed a significant proliferative response upon TSLP treatment. In addition, knockdown of TSLP in DCs or of TSLPR in $CD4^+$ T cells inhibited the differentiation and proliferation of $CD4^+$ T cells induced by *A. fumigatus*–stimulated DCs. Our data also confirmed that TSLP could polarize a Th17 inflammatory response and promote the worsening of FK in mice experiments. However, knockdown of TSLP obviously diminished the corneal injury induced by *A. fumigatus* infection. Thus, TSLP was involved in the regulation of both the innate and adaptive immune responses, and regulating TSLP may be a promising approach for moderating Th17 responses.

The JAK/STAT signaling pathway is a significant signaling transduction cascade of numerous cytokines that regulate the innate and adaptive immune responses.[37] JAK/STAT signaling is of paramount importance in regulating the development and differentiation of $CD4^+$ T cells into Th1, Th2, or Th17 cells. Previous findings from Shi et al.[38] suggested that blocking the JAK/STAT pathway restrained the inflammatory Th2 cell response induced by TSLP-DCs in allergic rhinitis. Taylor et al.[39] demonstrated that IL-6 and IL-23 induced the phosphorylation of STAT3 in neutrophils and that blockage of this pathway using JAK/STAT inhibitors impaired ROS production and hyphal killing in vitro and in FK. However, before this study, little research had been done on the molecular mechanisms of the JAK/STAT pathway linking $CD4^+$ T cells with *A. fumigatus* keratitis and TSLP. In the current study, high-throughput sequencing showed that JAK/STAT was the most remarkable signaling pathway in $CD4^+$ T cells co-cultured with *A. fumigatus*–stimulated DCs. We found that the JAK/STAT pathway could be activated by TSLP secreted by *A. fumigatus*–infected DCs and that the pathway eventually participated in a Th17-type immune response. Moreover, ruxolitinib (a JAK1/2 inhibitor) or BBI608 (a STAT3 inhibitor) significantly blocked the *A. fumigatus*–induced Th17 inflammatory response. In addition, knockdown of TSLP or TSLPR also disrupted the activation of the JAK/STAT pathway, which could be activated by exogenous rmTSLP treatment. The administration of ruxolitinib or BBI608 obviously suppressed the progression of FK

Investigative Ophthalmology & Visual Science

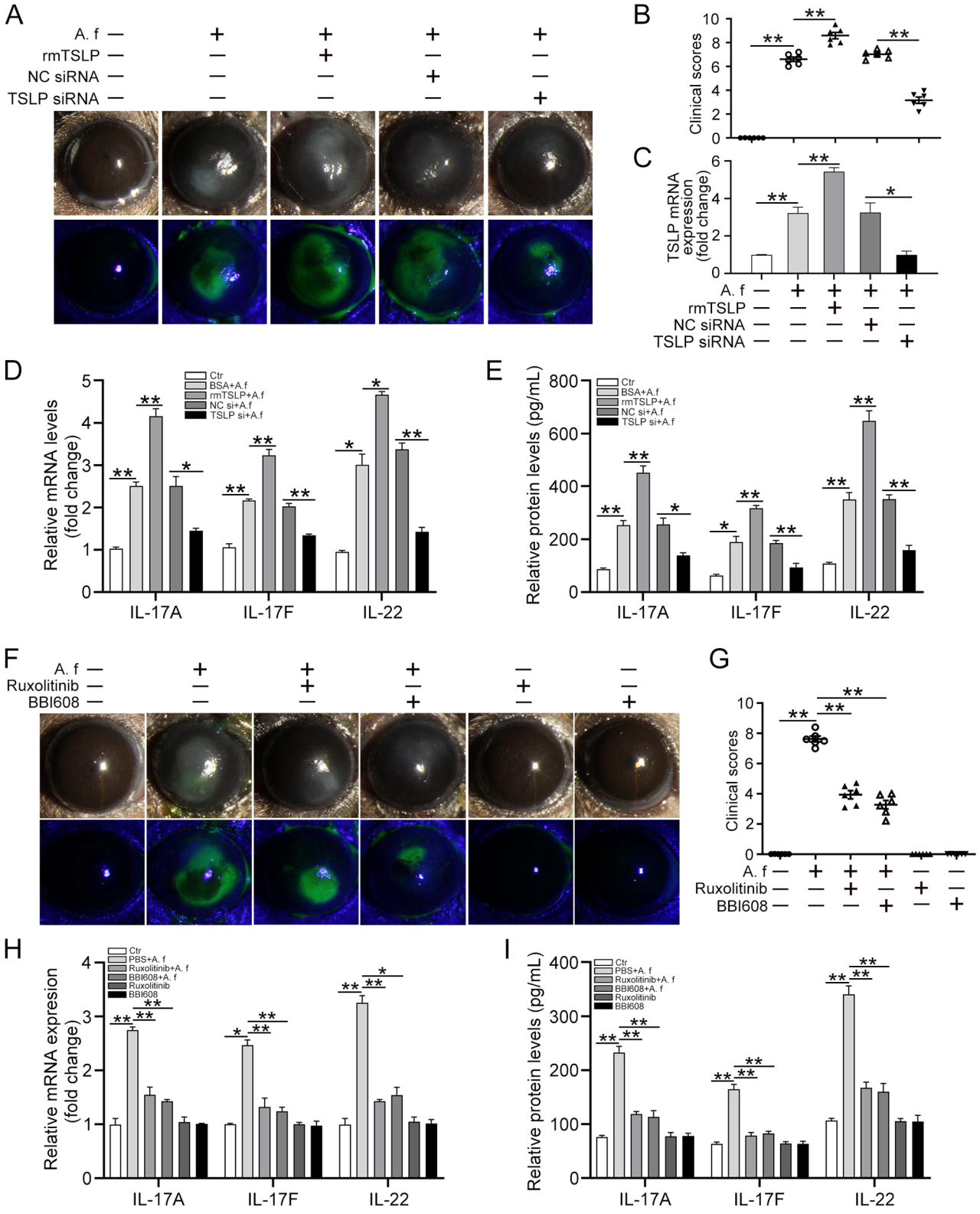

Figure 8. TSLP promotes FK progression through the JAK/STAT signaling pathway. C57BL/6 mice were pretreated by subconjunctival injection with 5 µL BSA, 5 µL rmTSLP (100 ng/µL), 5 µL NC siRNA, or 5 µL TSLP siRNA 1 day before infection with *A. fumigatus* hyphae (5 µL) for 1 day. (A) Slit-lamp examination was used to assess the clinical manifestation; fluorescein staining was performed to assess the denuded epithelium at 1 day after infection. (B) The average clinical scores were calculated to assess the clinical manifestation at 1 day after infection. (C and D) qRT-PCR was performed to detect the mRNA levels of TSLP, IL-17A, IL-17F, and IL-22 in mouse corneas at 1 day post infection. (E) ELISA was performed to detect the protein levels of IL-17A, IL-17F, and IL-22 in mouse corneas at 1 day after infection. The mouse eyes were subconjunctivally injected with PBS, 5 µL ruxolitinib (0.1 mmol/L), or 5 µL BBI608 (3 mmol/L) 1 day before infection

Investigative Ophthalmology & Visual Science

with *A. fumigatus* hyphae for 1 day. (F) Slit-lamp examination was used to assess the clinical manifestations and fluorescein staining was performed to assess the denuded epithelium at 1 day after infection. (G) The average clinical scores were calculated to assess the clinical manifestation at 1 day after infection. (H) qRT-PCR and (I) ELISA were performed to analyze the mRNA and protein levels of IL-17A, IL-17F, and IL-22 in mouse corneas at 1 day post infection. (Data are mean ± SEM, $^{*}P < 0.05$, $^{**}P < 0.01$, $n = 6$).

in the mice model of fungal infection. Therefore, targeted inhibition of the JAK/STAT pathway using specific inhibitors might represent a novel therapy for FK.

We have demonstrated that DCs served as a bridge between the innate and acquired immunities. DCs infected by *A. fumigatus* could drive naïve $CD4^+$ T-cell differentiation and trigger Th17 inflammatory responses in vitro and in vivo. Moreover, TSLP, secreted by *A. fumigatus*–stimulated DCs, acted as a significant molecule in the Th17-dominant immune responses of FK by activating JAK/STAT signaling. Our study expands the current understanding of the antifungal immune response and suggests novel therapeutic approaches for FK.

Acknowledgments

Supported by the National Natural Science Foundation of China (NSFC) (81470604 and 81770893).

Disclosure: **F. Han**, None; **H. Guo**, None; **L. Wang**, None; **Y. Zhang**, None; **L. Sun**, None; **C. Dai**, None; **X. Wu**, None

References

1. Sahay P, Singhal D, Nagpal R, et al. Pharmacologic therapy of mycotic keratitis. *Surv Ophthalmol*. 2019;64:380–400.
2. Mahmoudi S, Masoomi A, Ahmadikia K, et al. Fungal keratitis: an overview of clinical and laboratory aspects. *Mycoses*. 2018;61:916–930.
3. Yang H, Wang Q, Han L, et al. Nerolidol inhibits the LOX-1/IL-1beta signaling to protect against the Aspergillus fumigatus keratitis inflammation damage to the cornea. *Int Immunopharmacol*. 2020;80:106118.
4. Dai C, Wu J, Chen C, Wu X. Interactions of thymic stromal lymphopoietin with TLR2 and TLR4 regulate anti-fungal innate immunity in Aspergillus fumigatus-induced corneal infection. *Exp Eye Res*. 2019;182:19–29.
5. Tang Q, Che C, Lin J, et al. Maresin1 regulates neutrophil recruitment and IL-10 expression in Aspergillus fumigatus keratitis. *Int Immunopharmacol*. 2019;69:103–108.
6. Niu Y, Zhao G, Li C, et al. Aspergillus fumigatus increased PAR-2 expression and elevated proinflammatory cytokines expression through the pathway of PAR-2/ERK1/2 in cornea. *Invest Ophthalmol Vis Sci*. 2018;59:166–175.
7. Ren X, Wang L, Wu X. A potential link between TSLP/TSLPR/STAT5 and TLR2/MyD88/NFkappaB-p65 in human corneal epithelial cells for Aspergillus fumigatus tolerance. *Mol Immunol*. 2016;71:98–106.
8. Wolf AJ, Underhill DM. Peptidoglycan recognition by the innate immune system. *Nat Rev Immunol*. 2018;18:243–254.
9. Che CY, Yuan KL, Zhao GQ, et al. Regulation of lipoxygenase-1 and Dectin-1 on interleukin-10 in mouse Aspergillus fumigatus keratitis. *Int J Ophthalmol*. 2018;11:905–909.
10. Song J, Huang YF, Zhang WJ, Chen XF, Guo YM. Ocular diseases: immunological and molecular mechanisms. *Int J Ophthalmol*. 2016;9:780–788.
11. Hefter M, Lother J, Weiss E, et al. Human primary myeloid dendritic cells interact with the opportunistic fungal pathogen Aspergillus fumigatus via the C-type lectin receptor Dectin-1. *Med Mycol*. 2017;55:573–578.
12. Nguyen TNY, Padungros P, Wongsrisupphakul P, et al. Cell wall mannan of Candida krusei mediates dendritic cell apoptosis and orchestrates Th17 polarization via TLR-2/MyD88-dependent pathway. *Sci Rep*. 2018;8:17123.
13. Steger M, Bermejo-Jambrina M, Yordanov T, et al. beta-1,3-glucan-lacking Aspergillus fumigatus mediates an efficient antifungal immune response by activating complement and dendritic cells. *Virulence*. 2019;10:957–969.
14. Srivastava M, Bencurova E, Gupta SK, Weiss E, Loffler J, Dandekar T. Aspergillus fumigatus challenged by human dendritic cells: metabolic and regulatory pathway responses testify a tight battle. *Front Cell Infect Microbiol*. 2019;9:168.
15. Zhou L, Yao L, Zhang Q, et al. REGgamma controls Th17 cell differentiation and autoimmune inflammation by regulating dendritic cells. *Cell Mol Immunol*. 2019;17:834–842.
16. Patente TA, Pelgrom LR, Everts B. Dendritic cells are what they eat: how their metabolism shapes T helper cell polarization. *Curr Opin Immunol*. 2019;58:16–23.
17. Wang Y, Du X, Wei J, et al. LKB1 orchestrates dendritic cell metabolic quiescence and anti-tumor immunity. *Cell Res*. 2019;29:391–405.
18. Cosmi L, Maggi L, Santarlasci V, Liotta F, Annunziato F. T helper cells plasticity in inflammation. *Cytometry A*. 2014;85:36–42.
19. de Oliveira PG, Gomes CM, Avila LR, Ribeiro-Dias F, Leenen PJM, de Oliveira MAP. Dendritic cell line AP284 supports Th17 amplification. *Cell Immunol*. 2019;337:54–61.
20. Wang J, Sun W, Bond A, et al. A positive feedback loop between Th17 cells and dendritic cells in patients with endplate inflammation. *Immunol Invest*. 2019;48:39–51.
21. Liang Y, Yu B, Chen J, et al. Thymic stromal lymphopoietin epigenetically upregulates Fc receptor gamma subunit-related receptors on antigen-presenting cells and induces TH2/TH17 polarization through dectin-2. *J Allergy Clin Immunol*. 2019;144:1025–1035.e1027.
22. Zhao H, Li M, Wang L, et al. Angiotensin II induces TSLP via an AT1 receptor/NF-KappaB pathway, promoting Th17 differentiation. *Cell Physiol Biochem*. 2012;30:1383–1397.
23. Verstraete K, Peelman F, Braun H, et al. Structure and antagonism of the receptor complex mediated by human TSLP in allergy and asthma. *Nat Commun*. 2017;8:14937.
24. Park JH, Jeong DY, Peyrin-Biroulet L, Eisenhut M, Shin JI. Insight into the role of TSLP in inflammatory bowel diseases. *Autoimmun Rev*. 2017;16:55–63.
25. Wang L, Wang L, Wu X. Aspergillus fumigatus promotes T helper type 2 responses through thymic stromal lymphopoietin production by human corneal epithelial cells. *Clin Exp Ophthalmol*. 2016;44:492–501.
26. Wu TG, Wilhelmus KR, Mitchell BM. Experimental keratomycosis in a mouse model. *Invest Ophthalmol Vis Sci*. 2003;44:210–216.
27. Inaba K, Inaba M, Romani N, et al. Generation of large numbers of dendritic cells from mouse bone marrow cultures supplemented with granulocyte/macrophage colony-stimulating factor. *J Exp Med*. 1992;176:1693–1702.
28. Risitano AM, Peffault de Latour R. Ruxolitinib for steroid-resistant acute GVHD. *Blood*. 2020;135:1721–1722.
29. Yang L, Lin S, Xu L, Lin J, Zhao C, Huang X. Novel activators and small-molecule inhibitors of STAT3 in cancer. *Cytokine Growth Factor Rev*. 2019;49:10–22.

30. Zhai B, Wozniak KL, Masso-Silva J, et al. Development of protective inflammation and cell-mediated immunity against Cryptococcus neoformans after exposure to hyphal mutants. *mBio*. 2015;6:e01433–01415.
31. Wan Z, Zhou Z, Liu Y, et al. Regulatory T cells and T helper 17 cells in viral infection. *Scand J Immunol*. 2020;91: e12873.
32. Suryawanshi A, Cao Z, Thitiprasert T, Zaidi TS, Panjwani N. Galectin-1-mediated suppression of Pseudomonas aeruginosa-induced corneal immunopathology. *J Immunol*. 2013;190:6397–6409.
33. Taylor PR, Leal SM, Jr., Sun Y, Pearlman E. Aspergillus and Fusarium corneal infections are regulated by Th17 cells and IL-17-producing neutrophils. *J Immunol*. 2014;192:3319–3327.
34. Karthikeyan RS, Leal SM, Jr., Prajna NV, et al. Expression of innate and adaptive immune mediators in human corneal tissue infected with Aspergillus or fusarium. *J Infect Dis*. 2011;204:942–950.
35. Sun L, Chen C, Wu J, Dai C, Wu X. TSLP-activated dendritic cells induce T helper type 2 inflammation in Aspergillus fumigatus keratitis. *Exp Eye Res*. 2018;171:120–130.
36. Martinez-Lopez M, Iborra S, Conde-Garrosa R, et al. Microbiota sensing by Mincle-Syk axis in dendritic cells regulates interleukin-17 and -22 production and promotes intestinal barrier integrity. *Immunity*. 2019;50:446–461.e449.
37. Villarino AV, Kanno Y, O'Shea JJ. Mechanisms and consequences of Jak-STAT signaling in the immune system. *Nat Immunol*. 2017;18:374–384.
38. Shi Z, Jiang W, Wang M, et al. Inhibition of JAK/STAT pathway restrains TSLP-activated dendritic cells mediated inflammatory T helper type 2 cell response in allergic rhinitis. *Mol Cell Biochem*. 2017;430:161–169.
39. Taylor PR, Roy S, Meszaros EC, et al. JAK/STAT regulation of Aspergillus fumigatus corneal infections and IL-6/23-stimulated neutrophil, IL-17, elastase, and MMP9 activity. *J Leukoc Biol*. 2016;100:213–222.

Investigative Ophthalmology & Visual Science